RESEARCH ARTICLE

Paracoccidioides brasiliensis PbP27 gene: knockdown procedures and functional characterization

Isaura Torres[1,2], Orville Hernandez[1,3], Diana Tamayo[1,2], Jose F. Muñoz[1,2], Ana M. García[1], Beatriz L. Gómez[1,4], Angela Restrepo[1] & Juan G. McEwen[1,5]

[1]Unidad de Biología Celular y Molecular, Corporación para Investigaciones Biológicas (CIB), Medellín, Colombia; [2]Instituto de Biología, Universidad de Antioquia, Medellín, Colombia; [3]Grupo de Investigación en Biociencias, Facultad de Ciencias de la Salud, Institución Universitaria Colegio Mayor de Antioquia, Medellín, Colombia; [4]School of Medicine and Health Sciences, Universidad del Rosario, Bogotá, Colombia; and [5]Facultad de Medicina, Universidad de Antioquia, Medellín, Colombia

Correspondence: Isaura Torres, Carrera 72 A # 78B-141, Medellín, Colombia. Tel.: +57 4 4035950; fax: +57 4 441 5514; e-mail: isaurap10@gmail.com

Received 11 July 2013; revised 16 September 2013; accepted 20 September 2013. Final version published online 1 November 2013.

DOI: 10.1111/1567-1364.12099

Editor: Richard Calderone

Keywords
Paracoccidioides brasiliensis; Pb*P27*; p27; antisense RNA; gene silencing; fungal survival.

Abstract

Paracoccidioides brasiliensis PbP27 gene encodes a protein localized in both the fungal cytoplasm and cell wall. The parasitic infectious form produces this protein preferentially with the gene's expression varying between the fungus phylogenetic species. The biological function of the native p27 has yet to be determined during either growth of the yeast or host infection. Therefore, in this study, through the use of antisense RNA technology and *Agrobacterium tumefaciens*-mediated transformation, we generated mitotically stable *PbP27* mutants (*PbP27* aRNA) with the goal to evaluate the role of p27 in the biology and virulence of this fungus. *PbP27* expression was reduced 60–75% in mutants, as determined by real-time PCR in correlation with a decrease in p27 expression. No alterations in the growth curve or in the ability to shift from mycelia to yeast or from yeast to mycelia were observed in *PbP27* aRNA strains; however, we did observe a reduction in cell vitality. Moreover, a decrease in cell viability of *PbP27* aRNA yeast cells after interaction with IFN-γ-stimulated macrophages was detected. Based on these results, we propose that p27 plays a role in yeast cell architecture and represents one of the mechanisms employed by this fungus for its interaction with the monocyte/macrophage system.

Introduction

Paracoccidioides brasiliensis is a thermally dimorphic fungus and the causative agent of paracoccidioidomycosis (PCM), a chronic, systemic, and progressive disease that afflicts mostly men engaged in agriculture. This mycosis is peculiarly confined to Latin America (Brummer *et al.*, 1993; Restrepo & Tobón, 2009). Brazil constitutes the main endemic area and is followed at great distance by Colombia, Venezuela, Ecuador, Argentina, and other Latin America countries (Restrepo & Tobón, 2009). The disease is most likely caused by the inhalation of the conidia, propagules considered to be the infectious particles, which are produced by the fungus mycelial form when growing at temperatures below 26 °C. Once these particles reach the lungs, they undergo differentiation toward the parasitic yeast form (Restrepo *et al.*, 2001). For such reasons, the transition from conidia to yeasts cells is believed to be an essential virulence trait of this fungus (Restrepo & Tobón, 2009).

Various genes have been implicated in *P. brasiliensis* pathogenicity, especially regarding fungal survival and interaction with host cells (Mendes-Giannini *et al.*, 2008). Thus, the immunodominant antigen gp43 (Puccia *et al.*, 1986) has been found to protect against experimental infection in mice (Taborda *et al.*, 1998; Pinto *et al.*, 2000; Marques *et al.*, 2006). Other protective *P. brasiliensis* antigens capable of eliciting an effective immune response have been studied such as hsp60 (Cunha *et al.*, 2002), hsp70 (Bisio *et al.*, 2005), the 87-kDa antigen (Gomez *et al.*, 1997, 1998; Diez, 2004), a 45-kDa formamidase (Borges *et al.*, 2005), and the recombinant protein of

27 kDa (rPb27), present in the soluble fraction F0 (Reis *et al.*, 2008).

PbP27 was cloned and originally used as an immunological marker (McEwen *et al.*, 1996). The recombinant protein was used in ELISA, yielding values of sensitivity and specificity of 73.4% and 87.5%, respectively (Ortiz *et al.*, 1998). Subsequently, it was used in antibody detection (Ortiz *et al.*, 1996). Diez and coworkers profited from both p27 high specificity and 87-kDa high sensitivity to prepare an antigen cocktail and reported a sensitivity of 92% and a specificity of 88% when compared against normal human sera (Diez *et al.*, 2003).

The *PbP27* gene has no introns and possesses a single 660-bp coding region encoding a 220-amino acid protein (p27; www.broadinstitute.org/annotation/genome). Sequence analysis of the *PbP27* gene in different *P. brasiliensis* isolates, as well as in Pb01/*Paracoccidioides lutzii,* revealed that p27 is a highly conserved protein among all *P. brasiliensis* isolates assigned to the cryptic species S1, PS2, and PS3 that were tested with low variation between these isolates, but a divergent sequence concerning the Pb01/*P. lutzii* isolate (Matute *et al.*, 2008; Garcia Blanco *et al.*, 2011). The *PbP27* gene has evolved under a positive selection pressure showing patterns of adaptive evolution in this gene (Matute *et al.*, 2008).

The 27-kDa protein (p27) is expressed mostly in the yeast phase, and it is localized in the cell wall (Reis *et al.*, 2008; Garcia Blanco *et al.*, 2011). Reis *et al.* (2008) showed that mice immunization with rPb*27* prior to intravenous infection by the orbital plexus with a virulent *P. brasiliensis* (Pb18) isolate protected BALB/c mice. The authors also detected a high level of IgG isotypes and cytokines such as IFN-γ and TGF-β in response to the rp27 administrations, suggesting that this antigen contains T-cell, as well as B-cell, recognition epitope(s) (Reis *et al.*, 2008). Recently, other recombinant protein, rPb40, was used in association with fluconazole and shown to reduce fungal burdens in the lungs of BALB/c mice (Fernandes *et al.*, 2011, 2012).

To date, neither the biological function of p27 nor its potential role as a virulence factor has been characterized. For these reasons, we sought to evaluate (1) the presence of immunodominant and potentially protective human T-cell epitopes in the *PbP27* sequence, (2) the biological function of this protein, and (3) the behavior of *PbP27* knockdown yeast cells during their interaction with IFN-γ-stimulated macrophages. The results presented here indicate that p27 plays a role in the yeast cell architecture and has a crucial role during its interaction with the IFN-γ-stimulated macrophages perhaps by facilitating the persistence of the fungus inside the cells, thus allowing latency within the host tissues up to the moment when conditions favor its reemergence as a pathogen.

Materials and methods

Strains and culture conditions

Yeast strain

Paracoccidioides brasiliensis Pb339 (PbWt), a strain with capacity to produce host-recognizable antigens, was used for this study (Ortiz *et al.*, 1996; Gomez *et al.*, 1997; Diez *et al.*, 2003). Yeast cells were grown in brain–heart infusion (BHI) both solid and broth media (Becton Dickinson and Company, Sparks, MD) supplemented with glucose 1% and incubated at 37 °C in a shaker at 150 r.p.m. Morphological transitions from mycelium to yeast and germination from yeast to mycelia were carried out in BHI agar medium at 36 or 20 °C, respectively.

Bacterial strains

Plasmids were cloned and propagated in the *Escherichia coli* strain DH5α with growth at 36 °C in Luria–Bertani (LB) medium supplemented with appropriated antibiotics (Sambrook & Russell, 2001). *Agrobacterium tumefaciens* strain LBA1100 (Beijersbergen *et al.*, 1992) was used to carry the binary vectors used in this study; recombinant *A. tumefaciens* was maintained in LB medium supplemented with kanamycin (100 μg mL^{-1}).

T-cell epitope prediction

To identify immunodominant and potentially protective human T-cell epitopes in *PbP27*, we used the T-cell epitope prediction tool in the immune epitope database and analysis resource. This tool employs a consensus approach to predict MHC class II epitopes based upon predictive methods such as Sturniolo, ARB, and SMM_align. These methods combined allowed this prediction tool to calculate computationally an accuracy consensus prediction of T-cell epitopes (Wang *et al.*, 2010; Peters & Sette, 2007; Wang *et al.*, 2008). We focused on MHC class II proteins that present foreign peptides from extracellular pathogens, such as *P. brasiliensis,* to CD4+ helper (class II) T cells to initiate the immune response and searched for promiscuous epitopes capable of binding to multiple HLA molecules (Peters & Sette, 2007; Salimi *et al.*, 2010).

We selected twelve HLA-DR alleles that were frequent in the population, to ensure high prediction accuracy of the predicted peptides. These HLA-DR alleles were namely DRB1 0101, DRB1 0301, DRB1 0401, DRB1 0701, DRB1 1101, DRB1 1301, DRB1 0404, DRB1 0802, DRB1

0405, DRB1 1302, DRB5 0101, and DRB1 1501 (Iwai *et al.*, 2003, http://www.allelefrequencies.net/). Briefly, the prediction tool scanned the input amino acid sequence using 15-mer windows along and searched for each of the twelve HLA-DR alleles, a matrix of values for each amino acid residue at each position. The predicted tool provided a score for each one of the 15-mer windows along the scanned amino acid sequence (Wang *et al.*, 2010).

Plasmid construction, *P. brasiliensis* transformation and screening

The antisense RNA strategy and *A. tumefaciens*-mediated transformation (ATMT; Almeida *et al.*, 2009) were used to obtain an isolate with decreased *PbP27* gene expression. Four antisense oligonucleotides were designed based on the genomic sequence from Pb339 (GenBank accession number: U41503) reported by McEwen *et al.* (1996) as follows: AS1, base pairs 1–79 of *PbP27*; AS2, base pairs 51–159 of *PbP27*; AS3, base pairs 137–263 of *PbP27*; and AS4, base pairs 1–142 of *PbP27*. These fragments were individually inserted into the pCR35 plasmid under the control of the promoter region of the calcium-binding protein gene (CBP-1) from *Histoplasma capsulatum* (Rappleye *et al.*, 2004) and propagated in *E. coli* DH5α. Each *CBP*-1 promoter-AS cassette was subcloned into the pUR5750 plasmid, the parental binary vector to harbor the transferred DNA (T-DNA) with antisense molecules. As a Pb339 recombinant control, we used *P. brasiliensis* yeasts transformed with an empty vector (PbEV) as previously described (Almeida *et al.*, 2009; Hernandez *et al.*, 2010; Fig. 1a). Following transformation, cells were spread onto selective BHI media supplemented with hygromycin 100 μg mL^{-1} (Sigma-Aldrich, St. Louis, MO). Prior to incubation, plates were air-dried in a safety cabinet for 30 min. Selection plates were monitored for colony-forming ability at 36 °C for 15–20 days (Almeida *et al.*, 2009). To evaluate the phenotypic stability of the isolated *Agrobacterium*-mediated transformants, they were randomly selected and subcultured in liquid BHI containing 150 μg mL^{-1} hygromycin B for three consecutive times for 5 days at 36 °C and then evaluated again in solid medium with three biological replicates before their use in others assays.

Mitotic stability of transformants

The mitotic stability of the *P. brasiliensis* transformants was determined by analyzing the stability of hygromycin B resistance (Zhang *et al.*, 2011). Sixty hygromycin B-resistant transformants from the four antisense molecules were successively subcultured (five times) on BHI plates without hygromycin B. Then, the cells were subcultured in plates containing 150 μg mL^{-1} hygromycin (Zhang *et al.*, 2011).

Molecular detection of the hygromycin resistance gene (*HPH*)

Genomic DNA from PbWt, PbEV, and *PbP27* aRNA yeast cells was isolated according to the glass beads protocol described by van Burik *et al.* (1998). To confirm the presence of the hygromycin B resistance cassette, PCR amplification was carried out to detect HPH 1000-bp amplification product using primers *hphF* (5′-AACTC ACCGCGACGTCTGTCGA-3′) and *hphR* (5′- CTACACA GCCATCGGTCCAGA-3′). PCR included 30 cycles of 1 min at 94 °C for denaturing, 1 min at 68 °C for annealing, and 1.5 min at 72 °C for extension. The reaction products were analyzed in 1% agarose gel and visualized with ethidium bromide under UV light.

Total RNA extraction and real-time PCR analysis

Total RNA from PbWt, PbEV, and *PbP27* aRNA yeast cells was obtained using TRIzol® reagent according to the manufacturer's instructions (Invitrogen, Carlsbad, CA). Total RNA was treated with DNase I (Invitrogen). A conventional PCR using β-tubulin (Goldman *et al.*, 2003) primers was carried out to confirm the absence of chromosomal DNA. cDNA was synthesized using 1 μg of total RNA with SuperScript III reverse transcriptase according to the manufacturer's instructions (Invitrogen).

Real-time PCR (RT-PCR) was performed using Maxima® SYBR Green/Fluorescein qPCR Master Mix (2X), according to the manufacturer's instructions (Fermentas, MD). The CFX96 Real-Time PCR Detection System (Bio-Rad, Headquarters Hercules, CA) was used to estimate *PbP27* expression. β-tubulin was chosen as a housekeeping gene (Goldman *et al.*, 2003) to evaluate *PbP27* gene expression, whereas the ubiquitin (*UBI*) was used as a housekeeping gene to evaluate interleukin 6 (IL-6), IL-10, IL12p40, and tumor necrosis factor alpha (TNF-α) gene expression in the MH-S macrophage cell line (activated or not with IFN-γ) during interaction with *P. brasiliensis* strains at different time points (1, 3, 6, 12, 24, and 48 h). The primer sequences are described in Table 1. Melting curve analysis was performed after the amplification process to eliminate the possibility of nonspecific amplification or primer–dimer formation. Fold changes in mRNA expression were calculated using the $2^{\Delta\Delta C_T}$ formula, where $\Delta\Delta C_T$ is the difference between the target gene and β-tubulin (Livak & Schmittgen, 2001). Each experiment was carried out in triplicate, and the expression level was measured three times.

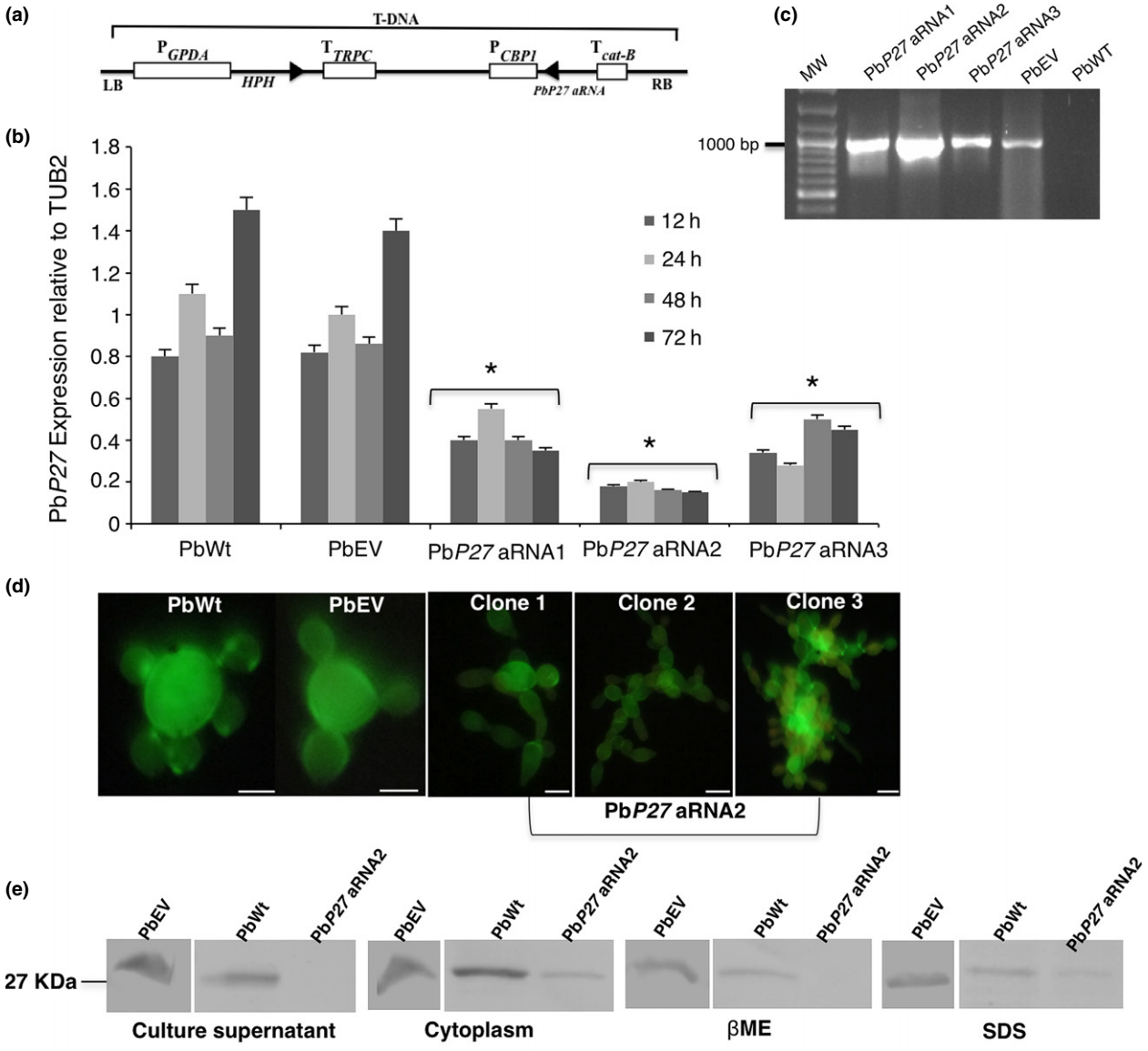

Fig. 1. *PbP27* knockdown using an aRNA plasmid and *Agrobacterium tumefaciens*-mediated transformation. (a) *PbP27* antisense cassette. Four antisense oligonucleotides were designed based on the genomic sequence from Pb339 reported by McEwen *et al.* (1996) as detailed in Materials and methods and cloned under the control of the *Histoplasma capsulatum CBP-1* promoter. The constructs were subcloned into the T-DNA region of the binary vector pUR5750 harboring the hygromycin B phosphotransferase (*HPH*) gene from *Escherichia coli*, driven by glyceraldehyde 3′-phosphate dehydrogenase gene promoter from *Aspergillus nidulans (P*GPDA*)*, and bearing transcriptional terminators Tcat-B and TRPC. (b) *PbP27* gene expression levels in PbWt, PbWt transformed with the empty vector (PbEV), and three *PbP27* aRNA clones (*PbP27* aRNA1, *PbP27* aRNA2, and *PbP27* aRNA3) after more than 18 months of subculture. Gene expression levels obtained by RT-PCR were normalized with the internal control *TUB2*; $*P < 0.05$ compared with PbWt and PbEV. (c) PCR fragments amplified with *HPH*-specific primers to yield a 1000-bp internal fragment. We used as template DNA from *PbP27* aRNA (clones 1, 2, and 3), PbWt, and PbEV. MW, DNA molecular marker. (d) *PbP27* aRNA2 (clones 1, 2, and 3) lost PbWt typical 'pilot wheel' morphology, showing a mother cell surrounded by elongated daughter cells, compared with control strains PbWt and PbEV, which showed rounded yeast cells. Cellular morphology of exponentially grown yeast cells was visualized by fluorescence microscopy using Calcofluor white staining. White bars correspond to 5 μm. (e) Immunoblots of four protein extracts from PbWt, PbEV, and *PbP27* aRNA2 yeast cells revealed with the anti-p27 monoclonal antibody (BJ4), βME: 2-mercaptoethanol.

Growth curve and vitality assays

Growth curves were performed in BHI broth (100 mL) inoculated with 48-h cultures (1×10^8 washed cells). Cellular density was measured in duplicates at 3, 6, 12, 24, 48, 72, 120, and 144 h of growth using a spectrophotometer.

Vitality was evaluated using the protocol reported by Hernandez (Hernandez *et al.*, 2010), which corresponds

Table 1. Peptides from p27 of *Paracoccidioides brasiliensis* with high-affinity recognition for most HLA-DR molecules evaluated

Number	Peptide	Sequence
1	P27 (39–53)	SGDPNRRTEDVDLVI
2	P27 (110–124)	QSWPQRPQYDLQTAT
3	P27 (155–169)	QGSRKEGTDIRDIIS
4	P27 (174–188)	AVPGKPELNFNQSQE

to the ability of yeast cells to metabolize glucose upon late activation of a cell membrane proton pump and subsequent acidification of the medium due to H^+ release. The acidification power in the presence of glucose is a good predictive test of yeast vitality (Kara *et al.*, 1987) because it allowed observing the physiological capabilities and metabolic functions of the cell. For that, PbWt, PbEV, and *PbP27* aRNA yeast cells were cultivated in BHI liquid medium and collected at 48 h of growth, washed twice with sterile water, pH 7.0, and suspended in a final volume of 8 mL of water (pH 7.0). Two milliliters of this suspension was added to a beaker containing 38 mL of water, and when the pH became stable (pH, 5.5–6), 10 mL of 20% glucose was added. The pH was recorded every three min for 1 h to evaluate the increase in supernatant H^+ levels. PbWt yeast cells treated with 16 μg mL^{-1} of amphotericin B (Fungizone, Bristol-Myers Squibb Pharmaceuticals, UK) during 4 h was used as a negative control of the assay. The assays were performed in triplicates.

Microscopy

The yeast cell morphology of PbWt, PbEV, and three different *PbP27* aRNA isolates (designated 1, 2, 3), generated with the same aRNA oligonucleotide (AS2), was evaluated. They were grown under standard conditions to exponential phase, collected and resuspended in 10 μL of a 10 μg mL^{-1} solution of Calcofluor white (Sigma-Aldrich), and observed using a Leitz Laborlux 11 fluorescence microscope provided with tungsten lamp, optic filters (340–380 nm) for UV light excitation, and a 40× objective. For image capture, we used a PowerShot G5 camera (Canon).

Translational evaluation of p27 expression

Preparation of yeast protein extracts

Protein extracts were obtained using a method previously described (Peñalver *et al.*, 1996; Gonzalez *et al.*, 2005), with minor modifications. Yeast cells were mixed with lysis buffer (100 mM Tris–hydrochloride pH 7.4, 1mM EDTA) containing 10% (v/v) protease inhibitor cocktail (Sigma-Aldrich). Culture supernatant fluid was recovered and dialyzed against distilled water at 4 °C and then concentrated by assisted evaporation to obtain the extracellular extract; at the same time, yeast cells were mechanically disrupted using glass beads and shaking in a vortex mixer (van Burik *et al.*, 1998). Cell breakage was assessed by microscopy examination. Cytoplasmic extract was obtained after sedimentation of debris containing proteins from membranes and cell wall (10 000 ***g*** for 30 min at 4 °C), washed three times and resuspended in PBS 10 mM, pH 7.4, containing 1% (vol/vol) of 2-mercaptoethanol (βME) plus protease inhibitor cocktail, and incubated at 37 °C for 30 min in a rotatory shaker. The cell wall was subsequently sedimented, and the supernatant fluid was recovered, dialyzed against distilled water at 4 °C, and concentrated by assisted evaporation (βME extract) until a 10-fold reduction in initial volume was achieved. βME-extracted walls were washed three times with chilled glass-distilled water and then boiled for 5 min with a 2% sodium dodecyl sulfate (SDS) solution in glass-distilled water. After treatment, the suspensions were centrifuged at 10 000 ***g*** for 15 min. The proteins eventually present in the supernatant were precipitated with 75% (vol/vol; final concentration) ethanol at 4 °C for 16 h. The precipitates were recovered by centrifugation at 9200 ***g*** for 30 min and suspended in water (SDS extract). Total protein concentration in the different samples was determined by the method of Bradford (Bradford, 1976).

SDS-PAGE and Western blot

SDS-polyacrylamide gel electrophoresis (SDS-PAGE) was performed basically as described by Laemmli (Laemmli, 1970). The different protein extracts obtained from PbWt, PbEV, and *PbP27* aRNA mutants were heat-concentrated in SDS-PAGE buffer under denaturing conditions and resolved in 12% gels. For Western immunoblot, the gel contents were transferred to 0.45-mm nitrocellulose membranes (Towbin *et al.*, 1979). Thereafter, membranes were blocked with 5% skim milk plus 1% BSA in a PBS solution containing 0.05% (v/v) Tween 20 (PBST) for 3h at room temperature and washed three times with PBST. The monoclonal antibody BJ4 (Diez, 2004) was diluted 1 : 1000 in PBST 5% skim milk plus 1% BSA and was used to identify the native 27-kDa protein, incubating for 2 h at room temperature. The membrane was then washed three times with PBST, and immunocomplexes were detected using peroxidase-conjugated AffiniPure goat anti-mouse IgG antibodies (1 : 1000 dilution in PBST 5% skin milk plus 1% BSA; Jackson Immuno-Research Laboratories, Inc.) incubated for 1 h at room temperature. The membranes were washed three times with PBST, and the reaction was developed in a fresh mixture of 4-chloro-1-naphthol (4C1N; Sigma-Aldrich)

and 3,3-diaminobenzidine tetrahydrochloride (DAB; Sigma-Aldrich); both suspensions were mixed, and H_2O_2 was added. The reaction was stopped with distilled water.

Antifungal activity of cell line MH-S activated with IFN-γ

A cell line (MH-S), which corresponds to mouse alveolar macrophages transformed with SV40, was obtained from the European Collection of Cell Cultures (ECACC No. 95090612). IFN-γ-activated alveolar macrophages were grown in RPMI 1640 medium supplemented with 2 mM glutamine (Invitrogen), 0.05 mM 2- mercaptoethanol (Sigma-Aldrich), and 10% fetal bovine serum (Invitrogen). For the assays, we used confluent monolayers obtained by adding 4×10^5 cells per well to 24-well tissue culture plates (Nunc, Kamstrup, Denmark) incubated for 24 h at 36 °C with 5% CO_2 prior to evaluating interaction with PbWt, PbEV, and *PbP27* aRNA2 yeast cells. Macrophage monolayers were activated for 18 h by adding recombinant IFN-γ to a final concentration of 10 μg mL^{-1} (BD PharMingen™) and incubated overnight at 37 °C under 5% CO_2. Nonactivated macrophages were used as an internal control of the experiment. The MH-S cells (activated and nonactivated with IFN-γ) were challenged with 8×10^4 yeasts per well diluted in 250 μL of complete RPMI medium and incubated at 37 °C for 1, 3, 6, 12, 24, and 48 h. After interaction, survival of *P. brasiliensis* yeast cells was evaluated using the CFU (colony-forming units) method. At each time point, cultures were rinsed with RPMI to remove free yeast cells (supernatant), distilled water was added to lyse IFN-γ activated and nonactivated macrophages, and then, PbWt, PbEV, and *PbP27* aRNA1 cells were removed. Dilutions of both suspensions (supernatant and intracellular/adhered fungi) were plated onto BHI plates supplemented with 0.5% glucose, 4% horse serum, and EDTA 300 mM and incubated at 37 °C for 5–8 days as previously described (Kurita *et al.*, 1993). The results obtained from the intracellular/adhered fungal suspension were compared with the number of yeast cells recovered in the supernatant, to control the number the yeast cells added to each well. Percentage of viable cells was expressed as the number of CFUs obtained from each experimental well (*P. brasiliensis* yeast cells with IFN-γ-activated alveolar macrophages) divided by the number of CFUs in the controls (*P. brasiliensis* yeast cells growing in RPMI serum without macrophage interaction). All experiments were performed by triplicate.

Statistics

Data are reported as mean ± standard error of the mean (SEM), and all assays were repeated at least three times. All statistical analyses were performed using SPSS STATISTICS 17.0 program with ANOVA. A P value ≤ 0.05 was considered statistically significant.

Results

P27 contains T-cell epitopes that exhibit high affinity for HLA-DR molecules

By means of the Web interface of the IEDB database resource, we analyzed the entire p27 amino acid sequence (220 aa) obtained from the BROAD Institute (PADG_08402 and PABG_07332 for *P. brasiliensis* strains Pb18 and Pb03, respectively). Using the consensus algorithm and the chosen twelve HLA-DR molecules, we obtained the peptides affinity score using the 15-mer windows. Prediction of promiscuous epitopes in p27 gave four peptide sequences with high affinity to eight different HLA-DR molecules, six of which revealed HLA-DR molecules shared by all four sequences (Fig. 2). The peptide *PbP27* 174–188 (AVPGKPELNFNQSQE) was predicted to be the most promiscuous ligand, while the peptide *PbP27* 155–169 (QGSRKEGTDIRDIIS) showed the highest affinity (Table 2).

PbP27 knockdown affects cell morphology and slightly impairs vitality, but not fungal growth

Using antisense (aRNA) technology and *A. tumefaciens* transformation, we generated *PbP27* aRNA strain to further study the role of p27 in *P. brasiliensis* (Almeida *et al.*, 2009; Hernandez *et al.*, 2010). We tested cassettes containing four different aRNA oligonucleotides (AS1, AS2, AS3, and AS4), which correspond to homologous sequence of *PbP27* (McEwen *et al.*, 1996) genetically engineered into T-DNA cassettes (Fig. 1a).

To further confirm decreased *PbP27* gene expression, we selected HygR transformants 1, 2, and 3 (Fig. 1b) and evaluated mRNA transcript levels by RT-PCR. A decrease in *PbP27* gene expression in the *PbP27* aRNA yeast cells was observed when compared with the control strains (PbWt) and the PbEV during a kinetics growth test (Fig. 1b). Yeast cells from the *PbP27* aRNA2 isolate, generated with aRNA oligonucleotide AS2, were chosen for further analysis due to the low level of *PbP27* gene expression as high as 70–75% that was confirmed after 18 months of successive subcultures.

After five subcultures in the absence of hygromycin B, all *P. brasiliensis* transformants grew on BHI containing 150 μg mL^{-1} hygromycin B, suggesting that *hph* gene was stably maintained in all transformants. Additionally, by means of a PCR using internal cassette primers, we tested the integration of the aRNA cassette in the transformants

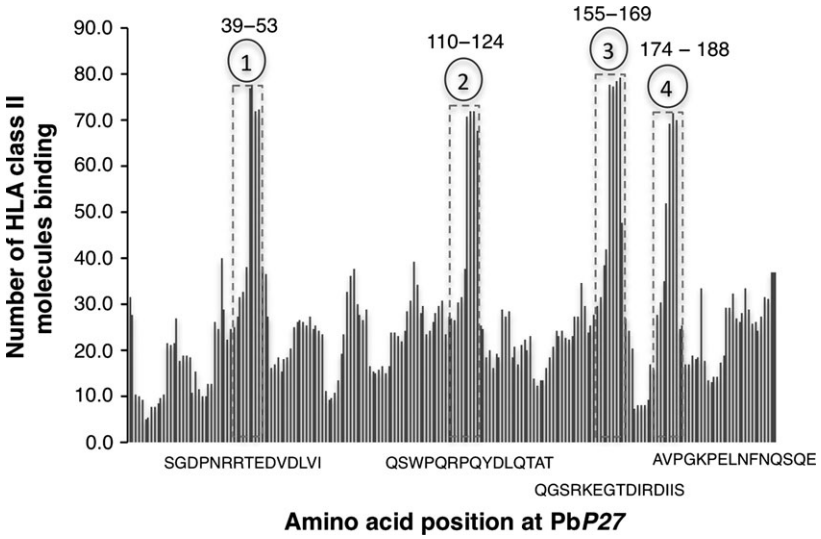

Fig. 2. Median affinity score value of p27 (220 aa) to 12 HLA-DR molecules. Bars placed in dashed line correspond to four peptides that show high-affinity recognition for most HLA-DR molecules included in the algorithm, which were selected as promiscuous epitopes.

Table 2. Oligonucleotide primer pairs used in RT-PCR

Primer name	Primer sequence 5′–3′
*PbP27*RT-F	CCTCGTGATCCATGTTGACCA
*PbP27*RT-R	TGTGCCCAAATTGGCTGACT
β-Tubulin-F	GTGGACCAGGTGATCGATGT
β-Tubulin-R	ACCCTGGAGGCAGTCACA
IL-6-F	ACACATGTTCTCTGGGAAATCGT
IL-6-R	AAGTGCATCATCGTTGTTCATACA
IL-10-F	TTTCAATTCCCTGGGGGAGAA
IL-10-R	GCTCCACTGCCTTGCTCTTATT
IL-12p40-F	CAAATTACTCCGGACGGTTCA
IL-12p40-R	AGAGACGCCATTCCACATGTC
TNF alpha-F	GCCACCACGCTCTTCTGTCT
TNF alpha-R	TGAGGGTCTGGGCCATAGAAC
Ubiquitin-F	TGGCTATTAATTATTCGGTCTGCAT
Ubiquitin-R	GCAAGTGGCTAGAGTGCAGAGTAA

growing in the selection media. In the strains with integrated cassettes and PbEV, a 1000-bp long fragment was observed, whereas no amplification product was observed when PbWt DNA was used as template (Fig. 1c).

Down-regulation of *PbP27* was accompanied by morphological alterations in cells transformed with the same aRNA oligonucleotide. These alterations were evaluated in three different *P. brasiliensis PbP27* aRNA isolates, generated with the same aRNA oligonucleotide (AS2), to check whether the random genetic insertion by ATMT might have disrupted genes involved in the morphological architecture of *P. brasiliensis* yeast cells.

Microscopic observation of cells stained with Calcofluor white allowed the identification of morphological alteration in *PbP27* aRNA isolates 1, 2, and 3, from the AS2 oligonucleotide, by fluorescence microscopy. The morphology in the PbWt and PbEV isolates (the last as PbWt recombinant control) revealed no apparent alteration in cellular morphology, and the typical round mother cell surrounded by multiple heterogeneous round daughter cells was observed (Fig. 1d). *PbP27* aRNA2 lost PbWt typical pilot wheel morphology, showing a mother cell surrounded by elongated daughter cells (Fig. 1d), condition that we related with a hard and clump colony in the culture medium of *PbP27* aRNA2 compared with soft colonies in the control strains (PbWt and PbEV). These alterations did not affect the growth rate (Fig. 3a), but did slightly decrease the ability of *PbP27* aRNA2 yeast cells to metabolize glucose (Fig. 3b). In addition, the low expression levels of *PbP27* did not alter the capacity for transition from mycelia to yeast nor the capacity for germination from yeast to mycelia (data not shown).

Inhibition of *PbP27* gene expression correlates with decreased p27 production

To verify whether p27 expression correlated with *PbP27* knockdown, we analyzed four yeast cell protein extracts from PbWt, PbEV, and *PbP27* aRNA2 yeast cells using immunoblots revealed with monoclonal anti-p27 antibody designated as BJ4 (Diez, 2004). We first followed p27 expression by immunoblot in PbWt protein extracts (culture supernatant, cytoplasmic, βME, and SDS extracts) and selected the extracts collected on day 7 for the next experiments, considering that day 7 represented the peak of p27 production in the cytoplasmic and SDS extracts (not shown). In the PbWt and PbEV protein extracts, p27 was mainly found in the cytoplasmic and SDS extracts, the latter containing cell wall proteins; a reduced amount of p27 was detected in the culture supernatant and βME extracts, in accordance with previous

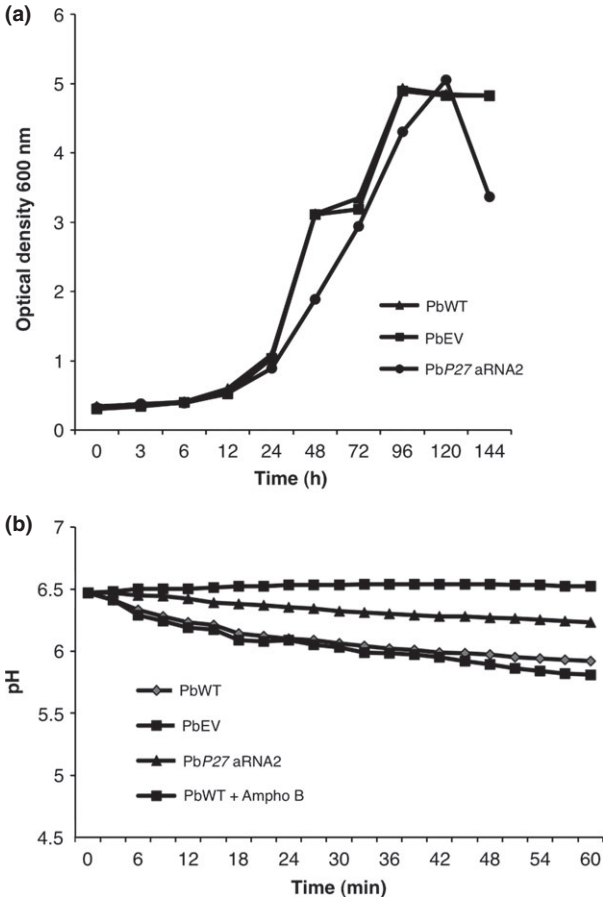

Fig. 3. Down-regulation of *PbP27* does affect growth curve and slightly the vitality of transformed *Paracoccidioides brasiliensis* yeast cells. Yeast-phase *P. brasiliensis* PbWt, PbEV, and *PbP27* aRNA2 were evaluated by (a) culture turbidity determined at an $OD_{600\ nm}$ and (b) culture medium pH during *in vitro* growth in BHI. PbWt yeast cells treated with 16 μg mL^{-1} of amphotericin B during 4 h were used as negative control of the assay. The assays were performed in triplicate.

reports (Reis *et al.*, 2008; Garcia Blanco *et al.*, 2011). Negligible p27 was detected in the same extracts from *PbP27* aRNA2 yeast cells (Fig. 1e).

Decrease in *PbP27* gene expression increased the susceptibility of *P. brasiliensis* yeast cells to IFN-γ-stimulated macrophages

To evaluate the effect of *PbP27* knockdown in *P. brasiliensis*, we challenged INF-γ-activated macrophages with PbWt, PbEV, and *PbP27* aRNA2 yeast cells. As determined by CFU, a decrease in recovery of the *PbP27* aRNA2 yeast cells from H_2O-washed macrophages was observed when compared with the PbWt and PbEV (Fig. 4a). Figure 4b shows CFU recovered from the supernatant, which was a control of the CFU recovered from *P. brasiliensis* and macrophages interaction and of

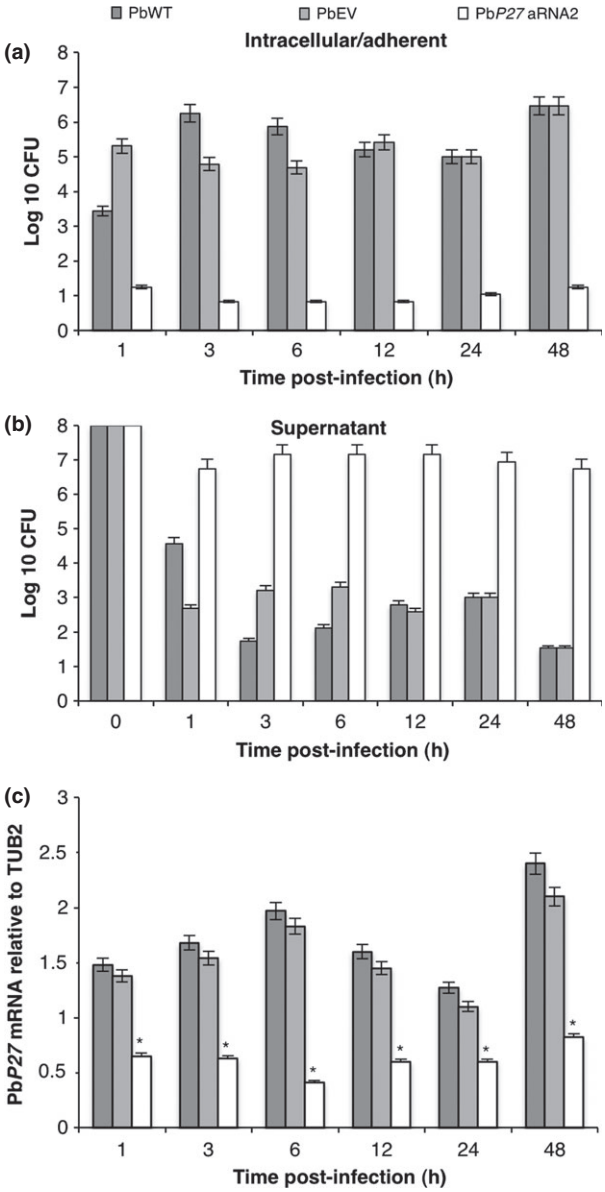

Fig. 4. Down-regulation of *PbP27* expression correlated with decreased recovery of intracellular/adhered yeasts from murine MH-S macrophages. (a) Recovered CFU from lysed IFN-γ-activated macrophages, (b) recovered CFU from supernatants of *Paracoccidioides brasiliensis*-infected culture macrophages, (c) gene expression levels of *PbP27* (relative to *TUB2*) during macrophage interaction assays with PbWt, PbEV, and *PbP27* aRNA2 yeasts. The periods evaluated were 0, 1, 3, 6, 12, 24, and 48 h after interaction (*$P < 0.05$ when compared with PbWt).

the quantity of yeast cells added in each experimental well. Additionally, we evaluated the *PbP27* gene expression level in PbWt, PbEV, and *PbP27* aRNA2 yeast cells during the interaction with IFN-γ-stimulated macrophages. *PbP27* expression was consistently reduced in the *PbP27* aRNA2 strain, both in the absence and in the

presence of activated macrophages, whereas PbWt and PbEV showed high expression level of *PbP27* predominantly at 48 h of the assay, independently of the presence or not of activated macrophages (Fig. 4c). In addition, gene expression levels of interleukins (IL) IL-6, IL-10, IL12p40, and TNF-α were not detected throughout the assays.

Discussion

The studies about p27 protein in *P. brasiliensis* have been framed in its use as a diagnostic tool (Ortiz *et al.*, 1996, 1998; Diez *et al.*, 2003) and during PCM pathogenesis using a recombinant protein (Reis *et al.*, 2008; Fernandes *et al.*, 2011). However, the role of native p27 in the cell biology and virulence of this fungus have not been explored. Therefore, in this study, with the use of antisense RNA technology, we obtained several mutants with down-regulation in *PbP27* gene expression and low levels of this protein in *P. brasiliensis,* to evaluate the role of p27 in the biology and virulence of this fungus.

The morphological alteration observed in yeast cells with low expression levels of this antigenic protein could be due to its localization as it has been demonstrated that p27 is mainly localized in cytoplasm and in the cell wall of *P. brasiliensis* yeast cells (Reis *et al.*, 2008; Garcia Blanco *et al.*, 2011). Similar effect was observed in different *PbP27* aRNA2 clones generated with the same aRNA oligonucleotide (AS2), which demonstrates that the reproducibility of the phenotypic alterations observed was due to the *PbP27* gene silencing and not a random gene disruption via genomic insertion by ATMT; in addition, no alterations were observed in the yeast transformed with the empty vector.

Previous works had reported the relation between morphology and virulence in *P. brasiliensis*. Almeida *et al.* reported that a reduction in the expression of Pb*CDC42* was associated with a homogenous cell shape and a reduced cell size, which makes the cell more susceptible to phagocytosis by macrophages and decreases its pathogenicity *in vivo* (Almeida *et al.*, 2009). In the same way, Hernandez *et al.* demonstrated that the down-regulation of Pb*HAD32* in *P. brasiliensis* induced alterations in morphology, and this alteration affected the yeast cells' capacity to adhere to human epithelial cells and decreased virulence *in vivo* (Hernandez *et al.*, 2010). Studies using interference RNA gene silencing strategy have reported that the silencing of *yps3* in *H. capsulatum* did not reduce virulence in a macrophage cell line *in vitro*, although their virulence was reduced during a mouse model of infection (Bohse & Woods, 2007). Here, we found that low expression levels of *PbP27* reduced the yeast cells capacity to metabolize glucose (vitality), but decreased even more of viability of *PbP27* aRNA2 yeast cells when they were exposed to IFN-γ-stimulated macrophages, which supports the idea that p27 represents one of the mechanisms that this pathogen uses to interact with the monocyte/macrophage system. Such interaction is believed to be important in the initial containment of the fungus (Calich *et al.*, 2008), that is, in permitting the *P. brasiliensis* uptake by host cells. Hence, p27 is one of a plethora of molecules that the fungus needs to protect it from being cleared by the host.

In our *in silico* analysis to determine T-cell epitopes, we found that *PbP27* possess 4 highly promiscuous peptides that are related to the 9 most prevalent HLA-DR molecules. This finding supports the results reported by Reis and collaborators who observed a high level of IgG isotypes and cytokines such INF-γ and TGF-β in response to rPb27, suggesting that this antigen contain T-cell as well as B-cell epitopes. Additionally, the immunization of BALB/c mice with rPb27 promoted a controlled pulmonary infection associated with low mortality rates, the presence of compact granuloma, and production of high levels of specific IgG2b (Reis *et al.*, 2008). That would be in agreement with the idea that p27 plays a role in the long periods of *P. brasiliensis* latency in the host, allowing survival of the fungus inside macrophages, as was confirmed in our study.

Pathogenic fungi have evolved mechanisms that permit evasion during primary infection or after the latency, which are useful in their intracellular pathogenic lifestyle. Positive selection has been found to play a role in the evolution of p27. Natural selection acting on *PbP27* might have had different outcomes, including (1) adaptation of a species to optimize the process of infection, (2) to escape host immune response and, as suggested by this work, to help its yeast cells to survive in macrophages and avoid their fungicidal activity, and (3) to inhabit different environmental niches (Matute *et al.*, 2008). Such considerations may help to interpret the observed behavior of knockdown isolates with decreased amounts of p27.

In this work, we have described several important aspects of the function of the native p27 protein that could give us a better understanding of the *P. brasiliensis* infectious process. In particular, the observations made here provide a basis for (1) an initial assessment of the biological function of the native p27 of *P. brasiliensis*, (2) a model of reproducibility and stability of the knockdown mutants targeting antigenic proteins, obtained by the technology based on aRNA and the transformation system mediated by *A. tumefaciens*, and (3) a model of intracellular pathogenic lifestyle of *P. brasiliensis* in a persistent infection inside IFN-γ-stimulated macrophages.

This is the first study to assess the effect of *PbP27* knockdown regulation in the biology of *P. brasiliensis* fungal cells and *in vitro* during its interaction with

IFN-γ-activated macrophages. However, future studies are needed to elucidate the possible immunomodulation pathway that p27 uses to allow *P. brasiliensis* to survive inside the macrophage and how its behavior could be related to the virulence of the fungus and the latency that characterizes PCM disease. Nevertheless, it is important to emphasize that fungal virulence is a polyvalent and complex process that requires the expression of multiple genes at different stages and at different sites of infection (Odds *et al.*, 2001). It does not depend on one single molecule. Hence, all research dedicated to studying virulence factor candidates and host–pathogen interaction mechanisms is called to solve this puzzle, in order to facilitate the understanding of *P. brasiliensis* virulence at the molecular level.

Acknowledgements

This work was supported by Colciencias project no. 221340820447. Support was also given by the Corporación para Investigaciones Biológicas and the Universidad of Antioquia through the fund of 'Sostenibilidad 2010–2011'. Colciencias' National Doctoral Program funding supported both I.T. and D.T.. We also acknowledge Professor Andrew Hamilton for allowing us to use the P27 monoclonal antibodies. The authors declare that they have no conflict of interest.

References

Almeida AJ, Cunha C, Carmona JA *et al.* (2009) Cdc42p controls yeast-cell shape and virulence of *Paracoccidioides brasiliensis*. *Fungal Genet Biol* **46**: 919–926.

Beijersbergen A, Dulk-Ras AD, Schilperoort RA & Hooykaas PJ (1992) Conjugative transfer by the virulence system of *Agrobacterium tumefaciens*. *Science* **256**: 1324–1327.

Bisio LC, Silva SP, Pereira IS, Xavier MA, Venancio EJ, Puccia R, Soares CM & Felipe MS (2005) A new *Paracoccidioides brasiliensis* 70-kDa heat shock protein reacts with sera from paracoccidioidomycosis patients. *Med Mycol* **43**: 495–503.

Bohse ML & Woods JP (2007) RNA interference-mediated silencing of the YPS3 gene of *Histoplasma capsulatum* reveals virulence defects. *Infect Immun* **75**: 2811–2817.

Borges CL, Pereira M, Felipe MS, de Faria FP, Gomez FJ, Deepe GS Jr & Soares CM (2005) The antigenic and catalytically active formamidase of *Paracoccidioides brasiliensis*: protein characterization, cDNA and gene cloning, heterologous expression and functional analysis of the recombinant protein. *Microbes Infect* **7**: 66–77.

Bradford MM (1976) A rapid and sensitive method for the quantitation of microgram quantities of protein utilizing the principle of protein-dye binding. *Anal Biochem* **72**: 248–254.

Brummer E, Castaneda E & Restrepo A (1993) Paracoccidioidomycosis: an update. *Clin Microbiol Rev* **6**: 89–117.

Calich VL, da Costa TA, Felonato M, Arruda C, Bernardino S, Loures FV, Ribeiro LR, de Cassia Valente-Ferreira R & Pina A (2008) Innate immunity to *Paracoccidioides brasiliensis* infection. *Mycopathologia* **165**: 223–236.

Cunha DA, Zancope-Oliveira RM, Sueli M, Felipe S, Salem-Izacc SM, Deepe GS Jr & Soares CM (2002) Heterologous expression, purification, and immunological reactivity of a recombinant HSP60 from *Paracoccidioides brasiliensis*. *Clin Diagn Lab Immunol* **9**: 374–377.

Diez S (2004) Characterization and use of serodiagnostically important antigens from *Paracoccidioides brasiliensis*. PhD Thesis, St. John's Institute of Dermatology, The Guy's, King's and St. Thomas' Medical School (KCL), University of London, London, pp. 121.

Diez S, Gomez BL, McEwen JG, Restrepo A, Hay RJ & Hamilton AJ (2003) Combined use of *Paracoccidioides brasiliensis* recombinant 27-kilodalton and purified 87-kilodalton antigens in an enzyme-linked immunosorbent assay for serodiagnosis of paracoccidioidomycosis. *J Clin Microbiol* **41**: 1536–1542.

Fernandes VC, Martins EM, Boeloni JN, Coitinho JB, Serakides R & Goes AM (2011) The combined use of *Paracoccidioides brasiliensis* Pb40 and Pb27 recombinant proteins enhances chemotherapy effects in experimental paracoccidioidomycosis. *Microbes Infect* **13**: 1062–1072.

Fernandes VC, Martins EM, Boeloni JN, Serakides R & Goes AM (2012) Protective effect of rPb40 as an adjuvant for chemotherapy in experimental paracoccidioidomycosis. *Mycopathologia* **174**: 93–105.

Garcia Blanco S, Munoz JF, Torres I, Diez Posada S, Gomez BL, McEwen JG, Restrepo S & Garcia AM (2011) Differential *PbP27* expression in the yeast and mycelial forms of the *Paracoccidioides brasiliensis* species complex. *Fungal Genet Biol* **48**: 1087–1095.

Goldman GH, dos Reis Marques E, Duarte Ribeiro DC *et al.* (2003) Expressed sequence tag analysis of the human pathogen *Paracoccidioides brasiliensis* yeast phase: identification of putative homologues of *Candida albicans* virulence and pathogenicity genes. *Eukaryot Cell* **2**: 34–48.

Gomez BL, Figueroa JI, Hamilton AJ, Ortiz B, Robledo MA, Hay RJ & Restrepo A (1997) Use of monoclonal antibodies in diagnosis of paracoccidioidomycosis: new strategies for detection of circulating antigens. *J Clin Microbiol* **35**: 3278–3283.

Gomez BL, Figueroa JI, Hamilton AJ, Diez S, Rojas M, Tobon AM, Hay RJ & Restrepo A (1998) Antigenemia in patients with paracoccidioidomycosis: detection of the 87-kilodalton determinant during and after antifungal therapy. *J Clin Microbiol* **36**: 3309–3316.

Gonzalez A, Gomez BL, Restrepo A, Hamilton AJ & Cano LE (2005) Recognition of extracellular matrix proteins by *Paracoccidioides brasiliensis* yeast cells. *Med Mycol* **43**: 637–645.

Hernandez O, Almeida AJ, Gonzalez A, Garcia AM, Tamayo D, Cano LE, Restrepo A & McEwen JG (2010) A 32-kilodalton hydrolase plays an important role in *Paracoccidioides brasiliensis* adherence to host cells and influences pathogenicity. *Infect Immun* **78**: 5280–5286.

Iwai LK, Yoshida M, Sidney J *et al.* (2003) In silico prediction of peptides binding to multiple HLA-DR molecules accurately identifies immunodominant epitopes from gp43 of *Paracoccidioides brasiliensis* frequently recognized in primary peripheral blood mononuclear cell responses from sensitized individuals. *Mol Med* **9**: 209–219.

Kara BV, Daoud I & Searle B (1987) European Bravery Convention, Proceedings of the 21st Congress, Madrid, 409.

Kurita N, Sano A, Coelho KI, Takeo K, Nishimura K & Miyaji M (1993) An improved culture medium for detecting live yeast phase cells of *Paracoccidioides brasiliensis*. *J Med Vet Mycol* **31**: 201–205.

Laemmli UK (1970) Cleavage of structural proteins during the assembly of the head of bacteriophage T4. *Nature* **227**: 680–685.

Livak KJ & Schmittgen TD (2001) Analysis of relative gene expression data using real-time quantitative PCR and the 2 (-Delta Delta C(T)) method. *Methods* **25**: 402–408.

Marques AF, da Silva MB, Juliano MA, Travassos LR & Taborda CP (2006) Peptide immunization as an adjuvant to chemotherapy in mice challenged intratracheally with virulent yeast cells of *Paracoccidioides brasiliensis*. *Antimicrob Agents Chemother* **50**: 2814–2819.

Matute DR, Quesada-Ocampo LM, Rauscher JT & McEwen JG (2008) Evidence for positive selection in putative virulence factors within the *Paracoccidioides brasiliensis* species complex. *PLoS Negl Trop Dis* **2**: e296.

McEwen JG, Ortiz BL, Garcia AM, Florez AM, Botero S & Restrepo A (1996) Molecular cloning, nucleotide sequencing, and characterization of a 27-kDa antigenic protein from *Paracoccidioides brasiliensis*. *Fungal Genet Biol* **20**: 125–131.

Mendes-Giannini MJ, Monteiro da Silva JL, de Fatima da Silva J, Donofrio FC, Miranda ET, Andreotti PF & Soares CP (2008) Interactions of *Paracoccidioides brasiliensis* with host cells: recent advances. *Mycopathologia* **165**: 237–248.

Odds FC, Gow NA & Brown AJ (2001) Fungal virulence studies come of age. *Genome Biol* **2**: REVIEWS1009.

Ortiz BL, Garcia AM, Restrepo A & McEwen JG (1996) Immunological characterization of a recombinant 27-kilodalton antigenic protein from *Paracoccidioides brasiliensis*. *Clin Diagn Lab Immunol* **3**: 239–241.

Ortiz BL, Diez S, Uran ME, Rivas JM, Romero M, Caicedo V, Restrepo A & McEwen JG (1998) Use of the 27-kilodalton recombinant protein from *Paracoccidioides brasiliensis* in serodiagnosis of paracoccidioidomycosis. *Clin Diagn Lab Immunol* **5**: 826–830.

Peñalver MC, O'Connor JE, Martinez JP & Gil ML (1996) Binding of human fibronectin to *Aspergillus fumigatus* conidia. *Infect Immun* **64**: 1146–1153.

Peters B & Sette A (2007) Integrating epitope data into the emerging web of biomedical knowledge resources. *Nat Rev Immunol* **7**: 485–490.

Pinto AR, Puccia R, Diniz SN, Franco MF & Travassos LR (2000) DNA-based vaccination against murine paracoccidioidomycosis using the gp43 gene from *Paracoccidioides brasiliensis*. *Vaccine* **18**: 3050–3058.

Puccia R, Schenkman S, Gorin PA & Travassos LR (1986) Exocellular components of *Paracoccidioides brasiliensis*: identification of a specific antigen. *Infect Immun* **53**: 199–206.

Rappleye CA, Engle JT & Goldman WE (2004) RNA interference in *Histoplasma capsulatum* demonstrates a role for alpha-(1,3)-glucan in virulence. *Mol Microbiol* **53**: 153–165.

Reis BS, Fernandes VC, Martins EM, Serakides R & Goes AM (2008) Protective immunity induced by rPb27 of *Paracoccidioides brasiliensis*. *Vaccine* **26**: 5461–5469.

Restrepo A & Tobón A (2009) *Paracoccidioides brasiliensis*. *Principles and Practice of Infectious Diseases*, 7th edn (Mandell B, Bennett J & Dolin R, eds), pp. 3357–3364. Elsevier, Churchill Livingston, Philadelphia.

Restrepo A, McEwen JG & Castaneda E (2001) The habitat of *Paracoccidioides brasiliensis*: how far from solving the riddle? *Med Mycol* **39**: 233–241.

Salimi N, Fleri W, Peters B & Sette A (2010) Design and utilization of epitope-based databases and predictive tools. *Immunogenetics* **62**: 185–196.

Sambrook J & Russell DW (eds) (2001) *Molecular Cloning: A Laboratory Manual*. Harbor Laboratory Press, Cold Spring, NY.

Taborda CP, Juliano MA, Puccia R, Franco M & Travassos LR (1998) Mapping of the T-cell epitope in the major 43-kilodalton glycoprotein of *Paracoccidioides brasiliensis* which induces a Th-1 response protective against fungal infection in BALB/c mice. *Infect Immun* **66**: 786–793.

Towbin H, Staehelin T & Gordon J (1979) Electrophoretic transfer of proteins from polyacrylamide gels to nitrocellulose sheets: procedure and some applications. *P Natl Acad Sci USA* **76**: 4350–4354.

van Burik JA, Schreckhise RW, White TC, Bowden RA & Myerson D (1998) Comparison of six extraction techniques for isolation of DNA from filamentous fungi. *Med Mycol* **36**: 299–303.

Wang P, Sidney J, Dow C, Mothe B, Sette A & Peters B (2008) A systematic assessment of MHC class II peptide binding predictions and evaluation of a consensus approach. *PLoS Comput Biol* **4**: e1000048.

Wang P, Sidney J, Kim Y, Sette A, Lund O, Nielsen M & Peters B (2010) Peptide binding predictions for HLA DR. DP and DQ molecules. *BMC Bioinformatics* **11**: 568.

Zhang Y, Li G, He D, Yu B, Yokoyama K & Wang L (2011) Efficient insertional mutagenesis system for the dimorphic pathogenic fungus *Sporothrix schenckii* using *Agrobacterium tumefaciens*. *J Microbiol Methods* **84**: 418–422.